Self-consistent turbulence in the two-dimensional nonlinear Schrödinger equation with a repulsive potential

Igor A. Ivonin
RRC Kurchatov Institute, 123182 Moscow, Russia

Vladimir P. Pavlenko
Department of Space and Plasma Physics, Uppsala University, S-755 91 Uppsala, Sweden

Hans Persson
Department of Space and Plasma Physics, Uppsala University, S-755 91 Uppsala, Sweden

(Received 3 February 1998; revised manuscript received 23 February 1999)

The dynamics of dark solitons (vortices) with the same topological charge (vorticity) in the two-dimensional nonlinear Schrödinger (NLS) equation in a defocusing medium is studied. The dynamics differ from those in incompressible media due to the possibility of energy and angular momentum radiation. The problem of the breakup of a multicharged dark soliton, which is a local decrease of the wave function intensity, into a number of chaotically moving vortices with single charge, is studied both analytically and numerically. After an initial period of intensive wave radiation, there emerges a *nonuniform, steady turbulent* self-organized motion of these vortices which is restricted in space by the size of the potential well of the initial multicharged dark soliton. Separate orbits of finite widths arise in this turbulent motion. That is, the *statistical probability* to observe a vortex in a given point has maxima near certain points (orbit positions). In spite of the fact that numerical calculations were performed in a finite region, the turbulent distributions of the vortices do not depend on the size of the container when its radius is larger than the size of the potential well of the primary multicharged dark soliton. The steady turbulent distribution of vortices on these orbits can be obtained as the extremal of the Lyapunov functional of the NLS equation, and obeys some simple rules. The first is the absence of Cherenkov resonance with linear (sound) waves. The second is the condition of a potential energy maximum in the region of vortex motion. These conditions give an approximately equidistant disposition of orbits of the same number of vortices on each orbit, which corresponds to a *constant rotating velocity*. The magnitude of this velocity is mainly determined by the sound velocity. An integral estimation of the self-consistent rotation of the vortex zone is given. [S1063-651X(99)08906-0]

PACS number(s): 47.10.+g, 47.32.Cc, 42.65.−k, 67.40.Vs

I. INTRODUCTION

The nonlinear Schrödinger (NLS) equation with a repulsive potential

$$i\Psi_t + \frac{1}{2}\Delta\Psi - U(|\Psi|^2)\Psi = 0 \tag{1}$$

describes [1] the propagation of modulated ion acoustic waves ($U=|\Psi|^2$), nonlinear waves in a waveguide with a ''normal'' dependence of the refraction index on the light intensity ($U=|\Psi|^2+\alpha|\Psi|^4$), the spatial diffraction of a laser beam passing through a diffraction grid and through a scattering material ($U=|\Psi|^2$), etc. This equation is also used to describe Bose condensate excitations [2–5].

Besides all this, there is an important Madelung transformation of this equation which leads exactly to the system of equations of gas dynamics. That is, separation of the real and imaginary parts in the complex equation (1) by $\Psi=\rho^{1/2}\exp(i\phi)$ results in $\rho=|\Psi|^2$ and the phase ϕ, corresponding to the density ρ and the potential of the velocity field $\vec{V}=\nabla\phi$ of a compressible medium:

$$\frac{\partial\rho}{\partial t} + \mathrm{div}(\rho\vec{V}) = 0,$$
$$\frac{\partial\vec{V}}{\partial t} + (\vec{V}\nabla)\vec{V} = -\nabla h, \quad \vec{V}\equiv\nabla\phi, \tag{2}$$

with the specific enthalpy

$$h = U(\rho) - \frac{\Delta\rho^{1/2}}{2\rho^{1/2}}. \tag{3}$$

This transformation of the NLS equation to gas dynamics equations creates the possibility to describe the behavior of NLS solutions in terms of sound waves and vortices despite the potential nature of the velocity $\vec{V}$. Indeed, to produce a single-valued field Ψ, one needs to have a velocity potential ϕ which is defined only up to a term $2\pi N$, where N is an integer. Thus, there are branch points or lines of ϕ corresponding to singular point vortices in the two-dimensional (2D) case and to singular vortex filaments in the 3D case. The field amplitude $|\Psi|$ must be equal to zero at the branch points. The velocity circulation around this branch point has the topological sense of an integer number of intersecting

zero lines of the real and imaginary parts of the field Ψ. It leads to the topological conservation of the frozen-in law. In particular, any vortex can disappear only due to collapse with a vortex having the opposite charge. Furthermore, a vortex cannot disappear during interaction with sound waves.

Thus the NLS equation gives one the possibility to *simulate quickly* the behavior of almost arbitrary vortex solutions and sound waves in *gas dynamic problems*, for solutions with a scale length greater than 1 (''healing length'' [4]). In this case the second term of the specific enthalpy is negligible. One can also include an arbitrary inhomogeneity in the potential energy U to describe an inhomogeneous medium. For example, it is possible to describe the nonuniform profile of the water depth H_0 in shallow water equations (in this case $U=\rho/H_0-1$).

In the 1D case, the NLS equation (1) is integrable when [6] $U=|\Psi|^2$, and has one parametric solution in the form of gray soliton (e.g., an exponentially localized density well). The amplitude of the modulation of gray solitons is determined by their velocity—a weakly modulated soliton propagates with the sound velocity, while a dark soliton (having a point with zero amplitude) is at rest. Like typical solitons, these gray solitons in the integrable 1D NLS equation can move through one another without changing their amplitude of modulation. But in the nonintegrable case, the gray solitons are attractors, [7], like typical solitons in a NLS equation with an attractive potential [8]. Thus gray solitons become visible during the evolution of an arbitrary initial distribution of the field Ψ, because the more modulated gray solitons increase their modulation due to interactions with small modulated solitons [7]. The attractive properties of gray solitons are saturated for some modulation level which is not necessarily equal to the maximum modulation of the dark solitons [7,9].

Moreover, a 1D NLS dark soliton becomes unstable with respect to 2D perpendicular perturbations [10]. Indeed, the 1D dark soliton has coinciding zero lines of both the real and imaginary parts of the field Ψ. Hence any small discrepancy of these lines leads to the generation of a 2D vortex street with alternating single intensities in places where zero lines intersect [3,10]. However, due to sound wave radiation, the vortex dipoles of this street may decrease their energy. This leads to a decrease of the distance l between the vortices, because the energy of a solitary vortex pair is proportional to $\ln(l)$, similar to that of the vortex dipole in hydrodynamics [11]. The velocity of a vortex dipole increases when the distance between vortices decreases. When this distance becomes equal to a critical value (which equals 2), the local sound speed (which equals $1/2^{1/2}$) is reached [12]. Then a collapse of this dipole in finite time occurs due to Cherenkov resonance, and the vortices disappear. This corresponds to a separation of the zero lines of the real and imaginary parts of the field Ψ. The energy radiation causing this separation leads to the disappearance of the holes $|\Psi|^2=0$ at the location of the collapse, and the density becomes smeared out. In other words, the zero lines move to infinity.

Thus any motion of vortices with different signs of the vorticity leads to their disappearance. Hence, in the 2D case the nontrivial long time behavior of vortices corresponds to a turbulent motion of vortices with the same sign of the vorticity.

Such motion can be observed [4] in a rotating container with He II, where vortices arise due to the nonideal corrections such as the impurity and the mutual friction of normal and superfluid components. In this case a regular (triangular) grid of *separate* vortices appears which rotates with the angular velocity Ω of the container [13]. Consequently, the uniform density w of the array of vortices and the average distance b between them is fully determined only by the container angular velocity Ω: $w\sim 1/b^2\sim\Omega$. The average distance b between the vortices is *much larger* than the quantum healing length, while the vortex velocities $V\sim 1/b\sim\Omega^{1/2}$ are much smaller than the sound speed in He II. Hence the motion of the vortices is fully determined by their coordinates, and is similar to the hydrodynamic motion of typical vortices in incompressible media. The 2D perturbations of the vortex positions in the grid may be treated as a kind of wave, the so called Tkachenko wave [13], with the phase velocity $V_{\vec{k}}\sim V\sim\Omega^{1/2}$ also determined only by the container angular velocity.

The distributions of vortices in a finite space region have been considered previously [14]. To analyze the stability of these distributions, the principle of the vortex free energy minimum (i.e., the energy integral in the rotating container coordinate system) was used. It was found that stable finite vortex distributions have a triangular grid similar to that in infinite space. *The averaged vorticity w* of this finite grid is uniform in space like that of the 3D stable hydrodynamic Kelvin vortex [11]. Vortex waves in such finite distributions also exist, but with some corrections due to the grid surface [15].

All above waves, which are perturbations of the vortex distribution, exist only within the grid and cannot radiate a vortex energy and angular momentum *outside* the grid. But if one takes radiation effects into account, i.e., finite compression or finite sound velocity, then the finite distribution of vortices will be unstable and expand due to the loss of vortex energy. This effect can be explained by the similarity between the vortex energy integral and the energy of a set of charged particles with the same electrical charges [11]. But the finite container size R may stabilize the vortex distribution spreading [11,12,16]. A sufficient criterion for *Lyapunov 3D stability* of the vortex distribution is the condition that the motion of the medium is subsonic in the coordinate system of rotating vortices. This can be obtained by Arnold's method of frozen-in variations [16]. This sufficient criterion of stability determines the minimum stable size $a_{\min}$ of the distribution of N vortices with a single $W=1$ vorticity flux (the velocity circulation). In the case $NW\ll RC_{s_0}$, corresponding to a large (compared to the healing length) distance between the vortices, this size $a_{\min}=(NWR/C_{s_0})^{1/2}\ll R$. Here C_{s_0} is the finite sound velocity of the background medium. Thus, a circular distribution of *separate* vortices, finite in space, with a *constant averaged vorticity* can be stable [4].

One should note that the size of the vortex region can be stabilized not only by the external container, but also by the ''extraordinary'' terms in the equation of state [similar to the second term in Eq. (3)]. For example, the ''extraordinary''

term in the specific enthalpy, which is inversely proportional to the square of the density, can stabilize the circular potential flow around a point with a zero value of the density. Indeed, in this case the flow is potential and subsonic everywhere around the hole, which is sufficient for the stability.

Another case of *initially nonseparate* vortices may arise when a multicharged vortex is broken. Indeed, this multicharged dark soliton (with total charge $N \gg 1$) has an unstable topology [17], because all the $2N$ zero lines of the real and the imaginary parts of the field Ψ intersect at one point. Due to this instability, this N-charged vortex is broken into a set of N singly charged vortices, that begin to move in the potential well of the primary vortex. Within this well the density $|\Psi|^2$ is much less than the background value, and the vortices are not separated, i.e., the distance between the vortices is of the order of the healing length.

In the above case of *nonseparate* vortices, there is no full hydrodynamic analogy, since the density well corresponds to a hydrodynamic hole (the absence of matter) only. No external parameters, such as the angular container velocity Ω or the radius R, can determine the distribution of vortices within the well. Only an internal parameter, the total number N of vortices, can determine all possible characteristics of this *turbulent*, inhomogeneous distribution.

In the present paper we investigate analytically and numerically the above case of self-consistent *turbulent* motion of nonseparate vortices. As a main result we have found numerically that *steady turbulent* vortex distributions appear in this *chaotic* vortex motion, and that they differ significantly from the *uniformly rotating* distribution of the hydrodynamic vortices in an incompressible medium. In particular, distinctly separate, but finite, width orbits of vortices with slightly increasing (with orbit number) distances between them have been obtained. Such a picture cannot be explained by any grid vortex distribution in which far orbits are not separated. The vortex distribution is approximately a constant number of vortices on each orbit. So the space averaged vortex density (vorticity) $w \sim 1/r$ differs from the case of a uniformly rotating Kelvin vortex. Thus it gives an approximately *constant distribution of the azimuthal (rotating) velocity* for the particular *nonseparate* vortices.

The value of the rotating velocity is mainly restricted by the phase velocity of the linear waves that corresponds to the absence of Cherenkov resonance. Indeed, the Cherenkov radiation carries energy and angular momentum out from the vortex zone during the initial period corresponding to the breaking of the multi-N charged dark soliton. The observed numerically *steady turbulent* state arises when the vortices occupy the region of the potential well of the primary multicharged dark soliton. The *statistical probability* to observe a vortex in a given point can be obtained as the extremal of some functional subject to NLS integrals of motion. In the paper we obtain this functional and the equation for its extremal. The self-consistent rotation of a particular distribution and the total number of orbits are indeed determined only by the total number of vortices, and do not depend on the container angular velocity and radius. From an analysis of this Lyapunov functional we also found that the simple criterion of the most stable distribution is a maximum of the potential energy in the vortex zone.

The analytical solution of the equation for the extremal allows us to explain some features of the numerically observed turbulence (the orbit positions and the value of the self-consistent rotation). We have done this analytically in the *most simple way*, assuming a zero width of the orbits, which roughly corresponds to the mean-field approximation. We have found that some features of the numerically observed turbulence (the orbit positions) are in good agreement with our analytical mean-field approximation, whereas the others (the integral estimations of the self-consistent rotation and the density level) do not coincide. This deviation is due to the correlations of the vortex positions, which are not taken into account in the simplified analytical model of the mean field.

II. STEADY STATE TURBULENT VORTEX DISTRIBUTIONS

Here we analyze the self-organized turbulent motion of 2D vortices which arises due to the breakup of a multicharged NLS dark soliton (with charge $N \gg 1$). Let us consider Eq. (1) with the simplest nonlinearity,

$$U(|\Psi|^2) = |\Psi|^2 - 1, \tag{4}$$

where the usual infinite boundary condition $|\Psi|^2 \to 1$ corresponds to a constant background. The phase dependence of the field Ψ at infinity is not determined by this condition. We will consider the phase dependence $\Psi \to \exp(iN\theta)$, with N zero lines of the real part and N zero lines of the imaginary part of the field Ψ at the *infinity*. According to Eqs. (2), this asymptotic value corresponds to a finite value of the velocity circulation $\oint \vec{V} d\vec{l} = 2\pi N$ at infinity. Thus the conditions chosen describe N singular vortices (dark solitons) located in the branch points of the field Ψ, with the total vorticity (charge) equal to N.

Let us first consider the multicharged dark soliton solution of Eq. (1), which has the form

$$\Psi(\vec{r},t) = \Psi_0(r)\exp(iN\theta). \tag{5}$$

Then, the amplitude $\Psi_0(r)$ for the particular potential (4) is defined by

$$\frac{1}{2r}(r\Psi_0')' + \left(1 - |\Psi_0|^2 - \frac{N^2}{2r^2}\right)\Psi_0 = 0. \tag{6}$$

The solution of Eq. (6) cannot be expressed analytically, but has the following asymptotic forms for $\Psi_0(r)$:

$$\Psi_0(r) \to 1 - \left\{\frac{N}{2r}\right\}^2, \quad r \to \infty,$$

$$\Psi_0(r) \to \alpha r^N, \quad r \to 0, \tag{7}$$

where the value α is the solution of the boundary value problem described by Eqs. (6) and (7). An approximate value of α can be obtained from the condition of smooth behavior of $\Psi_0(r)$ at some intermediate inflection point $r = a$:

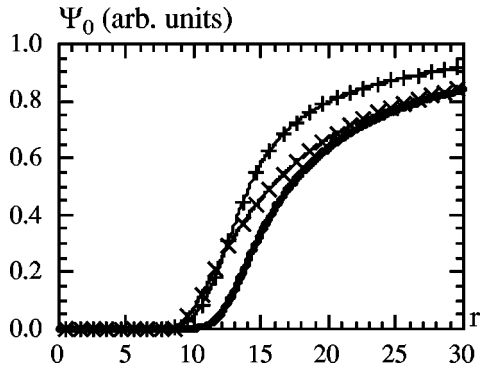

FIG. 1. Radial dependence of the dark soliton solution $\Psi_0(r)$ for $N=17$ (curve with + signs) and the potential well $|\Psi_0|^2$ (smooth curve). The approximate form (7) for this potential well (curve with $\times$ sign) is also shown.

$$\alpha=\frac{1}{(1+0.5N)a^N},$$

$$a=\frac{N}{2}\left(1+\frac{2}{N}\right)^{1/2}. \tag{8}$$

For example, for $N=17$, the exact value of $\alpha\approx 2.90\times 10^{-20}$ is only 1.6 times greater than the one estimated from Eqs. (8). In Fig. 1 we plot the numerical solution of this boundary value problem to show the typical form of potential well $|\Psi_0|^2$, and to demonstrate that the value $a\approx 9$ obtained from Eq. (8) indeed approximately corresponds to the position of the potential well edge $a_b\approx 10$ estimated through the position of tangent line in the inflection point of the $\Psi_0(r)$ curve.

The multicharged dark soliton has an unstable topology. Indeed, from Fig. 1 one can see that everywhere inside the potential well $\Psi_0^2(r)$ the value of potential is very small; it increases monotonically, and can reach the value ≈ 0.01 only when $r\approx a$. Thus any small perturbations of the field $\Psi(\vec{r})$ result in the appearance of additional zeros of Ψ^2. The whole set of weakly perturbed solutions Ψ in this potential well can be described by Eq. (1), linearized on a zero background $|\Psi_0|^2\approx 0$:

$$i\Psi_t+\tfrac{1}{2}\Delta\Psi+\Psi=0, \quad r<a. \tag{9}$$

All possible solutions of this linear equation are free waves within the well. The intersections of zero lines of the real and imaginary parts of the field Ψ may correspond to the vortex positions. The solutions of the linear Schrödinger equation (9) with given frequencies and boundary conditions at the edge of the circular potential well are Bessel functions. Thus the radial distribution of the vortices has a number of separate orbits corresponding to the zeros of the Bessel functions. The distance between these orbits is approximately constant. This can be seen from the dispersion relation obtained from Eq. (9): $\omega_{\vec{k}}=\vec{k}^2/2-1$. For stationary perturbations we have $\omega_k=0$; thus we find that the corresponding distance between the zeros of Ψ equals $\lambda/2=\pi/2^{1/2}\approx 2.2$. A more accurate calculation below gives some increase (with the orbit number) of this distance between consecutive zeros.

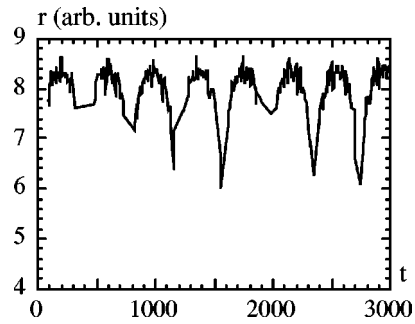

FIG. 2. Radius of the most distant single vortex vs time in the distribution of $N=13$ vortices.

To support the analytical prediction above, we have made a numerical simulation of the NLS equation (1). Our numerical simulations were made using the finite difference method ''predictor-corrector'' of second order accuracy in time and space in order to find intersections of the zero lines of the real and the imaginary parts of field Ψ in the simplest way (by direct calculation of the velocity circulation near these points). It should be noted here that for problems where the the exact positions of vortices are not needed, one can use faster algorithms, e.g., the ''split-step'' method or the method of polynomial expansion [2]. These numerical methods of solution of the NLS equation conserve both all possible frozen-in integrals and the usual hydrodynamic integrals of the mass M, energy E, momentum $\vec{P}$, and angular momentum $\vec{M}$:

$$M=\int (|\Psi|^2-1)d^2r,$$

$$E=\int \frac{1}{2}(\nabla\Psi)^2+\frac{1}{2}(|\Psi|^2-1)^2d^2r,$$

$$(\vec{M})_z=\frac{i}{2}\int [\vec{r}\times(\Psi^*\nabla\Psi-\Psi\nabla\Psi^*)]_z d^2r, \tag{10}$$

and can be used successively for fast solution of the equations of gas dynamics (2). Our numerical method conserves exactly the mass integral only. The relative perturbations of the angular momentum and energy integrals do not exceed 0.5% and 1.5%, respectively, during the whole time of the numerical simulations. The numerical simulations of the NLS equation (1) with the potential (4) were made in a container with a large (in comparison with the size of the vortex zone) radius. Only the absence of the normal component of the velocity field at this boundary is assumed in the numerical simulations.

Figure 2 demonstrates an example of this numerical simulation of the breakup of the multicharged dark soliton with $N=13$. This picture shows the radial position of the most distant single vortex versus time. The boundary (container) radius in this simulation was $R=50$. From this figure one can see that the size of the vortex zone is less than about 8.5, and is determined mainly by the radius a of the potential well of the initial multicharged soliton [$a\approx 7$ according to Eq. (8)]. The best fitting of the above radial position as a power of time gives the value zero (with the accuracy 0.001). This corresponds to at least a 40 times slower rate of expansion of

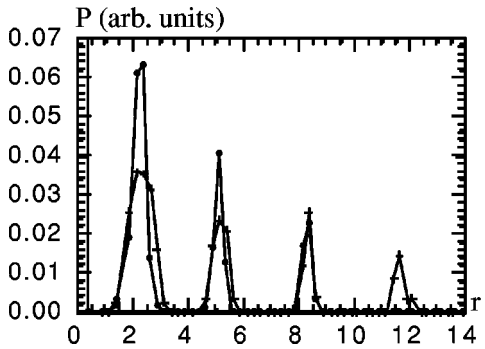

FIG. 3. Numerically obtained steady state turbulent radial distributions of the probability $P(r)$ to detect a vortex at radius r. This distribution of probability $P(r)$ has maxima corresponding to the orbit positions. This distribution consists of $1+4+4+4$ (curve with points) and $1+4+4+4+4$ (curve with + signs) vortices for the cases $N=13$ and 17, respectively. The orbit positions coincide, but a new orbit arises in the case $N=17$.

the vortex zone, compared with the rate $\gamma_a=0.5/(N+1)=0.04$ of purely acoustic, separate vortices [18]. Hence not all gas dynamic analogies can be applied to the particular problem. The same vortex zone size was also obtained in the case $R=25$ of the container radius. Thus, the container cannot influence significantly the size of the vortex zone.

The total time ($T=3000$) of the numerically observed evolution was at least 100 times larger than the time scale $t_c \sim a$ of the motion of a single vortex within the vortex zone. For example, the breakup of the initial unstable multicharged vortex finished at $t_b \approx 50$. The main features of the turbulent distribution are established in at least a time *ten times smaller* than the time of observation. Thus we indeed have a steady turbulent motion of the vortices in the vortex zone with a restricted spatial size.

The relatively short time periods when the radius of the vortex zone decreases to the value ≈ 5.5 may correspond to the Fermi-Pasta-Ulam chain phenomenon because of the small nonlinearity of the NLS equation in the vortex zone. These short time periods do not significantly influence the turbulent distribution of vortices.

It is worth noting here that linear waves with classical wavelengths greater than the healing length $\lambda > \pi 2^{0.5}$ cannot be radiated outside the vortex zone. This is because these waves have a negative frequency inside the vortex zone, whereas all outgoing sound waves outside the vortex zone must have a positive frequency. The absence of such radiation can also be explained by the the acoustic model of an inhomogeneous medium. Indeed, in the classic consideration a vortex region of the particular problem corresponds to a hole with finite size, and the reflection of the waves from the boundary of the vortex zone must be almost perfect. Thus, similar to the absence of radiation in the electrons in an atom, there is no reason to expect any outgoing radiation from the dark solitons that move chaotically in the vortex region. This may explain the stability of the vortex distributions in the presented numerical experiments.

Let us now consider these distributions of vortices within this vortex zone. Two particular examples (for $N=13$ and 17) of the radial distribution of the probability $P(r)$ to detect a vortex at the radial position r are presented in Fig. 3. One can see that these probabilities have a nonmonotonic character with approximately coinciding maxima, i.e., the separate orbits arise in the chaotic motion of vortices. In both cases there is also a single vortex in the position $r \approx 0$ with a singular density. There are three orbits (with distribution $13=1+4+4+4$) for $N=13$, while for $N=17$ there are four orbits (with distribution $17=1+4+4+4+4$). We can compare these numerical results with the solutions of the linearized equation (9). The steady state solution of this equation within the first orbit is determined mainly by the central single vortex. Thus the appropriate solution will be the Bessel function $J_1(2^{1/2}r)$ with its first zero at the point $(2^{1/2}r)=3.8$, corresponding to the first orbit position $r_1=2.7$. This value approximately equals the one obtained numerically. Then, between the first and second orbits, the solution is determined by five vortices, which can be described by a linear combination of the Bessel functions of fifth order, $J_5(2^{1/2}r)$ and $Y_5(2^{1/2}r)$, with coefficients satisfying the conditions to be equal to zero at the position of the first orbit and to have smooth behavior in the vicinity of this position. The position of the next zero of this combination is mainly determined by first zero $J_5(2^{1/2}r)$, and corresponds to the second orbit position $r_2 \geqslant 6.2$. This value is a little greater than the numerically obtained value $r_2 \approx 5$. In some calculations (for example, in case $N=11$), we have not found any vortex in the central position (the appropriate distribution is $11=0+4+4+3$). In this case the first orbit position ($r_1 \approx 1$) differs significantly from those in the $N=13$ and 17 distributions, but is mainly determined by the first zero of $J_0(2^{1/2}r)$, which corresponds to $r_1=1.7$.

Thus we can describe the turbulent distribution of vortices using the steady state solution of the linearized equation (9), although there is some deviation in orbit positions, namely, the numerically obtained distributions are more compact. But we will demonstrate that this deviation can be reduced by taking into account the self-consistent rotation of the steady state solutions of Eq. (9).

The particular distributions differ significantly from the triangular grid distribution of *separate* hydrodynamics vortices [14] in superfluid He II. For example, the triangular grid has the following distributions for particular number of vortices: $N=11=3+8$, $N=13=4+9$, $N=17=1+5+11$, and $N=\infty=1+7+19+37+\cdots$. These distributions correspond to a uniform rotation (with container angular velocity) of the vortex grid. Hence the distributions of separate point vortices have a uniform vortex density (vorticity or curl of velocity).

To understand the reason for this difference between the distributions of *separate* and *nonseparate* vortices, in Fig. 4 we show the azimuthal and radial velocities that arise in the vortex zone in the numerical simulation for $N=17$ *nonseparate* vortices. One can see that the azimuthal velocity has approximately a uniform profile in this zone.

Taking into account the potential (4) in Eq. (1), and linearizing this equation on the background $|\Psi|^2=1$, one can obtain [2] the phase velocity of linear waves away from vortices, $V_{\vec{k}}=[1+(\vec{k}^2/4)]^{1/2}>1$. Thus to avoid Cherenkov resonance with sound waves any vortex in a stable distribution should not move with a velocity exceeding the background sound speed $C_{s_0}=U'_\rho(\rho)=1$. But the local sound speed $C_s^2 \equiv \rho+(\Delta\rho^{1/2}/4\rho^{1/2})$ [12] can be both less than C_{s_0} (due to the

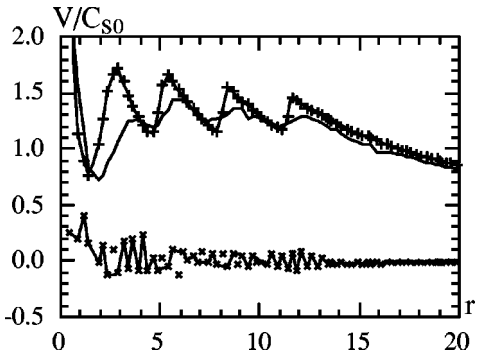

FIG. 4. Radial dependence of the averaged azimuthal (smooth curve) and radial (curve with $\times$ signs) velocities V/C_{s_0} (normalized to the background sound velocity C_{s_0}) arising in the vortex zone in the numerical simulation for $N=17$. The curve with $+$ signs is the azimuthal velocity that was obtained from the vortex distribution from Fig. 2.

decrease of the density $|\Psi|^2$) and greater than C_{s_0} (due to the inhomogeneity of the density near the vortex). For example, a dipole vortex begins to collapse when the velocity of the vortex pair exceeds the local value of the sound speed [12] $1/2^{1/2}$. Thus in our case some discrepancy from the hydrodynamic stability rule $V<C_{s_0}=1$ may also arise.

Starting from the first orbit position, the value of the azimuthal velocity is restricted mainly by the background sound velocity $C_{s_0}=1$, i.e., by the minimum possible phase velocity of linear waves, which can carry out energy and angular momentum from the vortex zone. Since the turbulent motion is a steady state turbulent one, the radiation of energy and angular momentum due to the Cherenkov radiation must be prohibited. This corresponds to the azimuthal velocity $V_\theta(r)\leqslant C_{s_0}=1$ and the averaged vortex density $w(r)=1/r$ [for $V_\theta(r)=1$]. Then the total number of vortices on each orbit becomes $N_i=w(r_i)r_i\delta r_i=\delta r_i$, i.e., the distance between ith and $(i+1)$th orbits, which is approximately constant. Thus, indeed, the observed distribution of constant velocity of the *nonseparate* vortices can be explained by the absence of Cherenkov resonance.

A more precise solution (which takes into account the self-consistent rotation of the vortex zone) of the preferred vortex distribution can be obtained by means of the Lyapunov functional. This functional looks like vortex free energy [14], but does not depend on the container angular velocity. Indeed, let us consider the functional F consisting of nontrivial integrals (10) of the particular problem

$$F=E+\Omega_N(\vec{M})_z+CM, \tag{11}$$

where Ω_N and C are Lagrange multipliers. The kinetic part of the energy integral E in this functional diverges at infinity. But for the Lyapunov principle, only the convergence of variations of the functional is required. Thus to avoid divergence one can calculate the variation of this functional from some solution of Eq. (1) with the particular boundary conditions $\Psi\rightarrow\exp(iN\theta)$. For our purposes, it is convenient to calculate the variation of this functional from the initial solution in the form of a dark soliton [Eq. (6)] or from its approximate expression given by Eq. (7).

The first variation of F with integrals (10) for arbitrary variations of Ψ and Ψ^* is zero if

$$i\Omega_N\Psi'_\theta+\frac{1}{2}\Delta\Psi+(1-|\Psi|^2)\Psi=C\Psi. \tag{12}$$

The extremal solution of Eq. (12) has the particular asymptotic form $\Psi\rightarrow\exp(iN\theta)$ at infinity only when $C\equiv-N\Omega_N$. To determine the second constant Ω_N (which has the sense of the angular velocity of the vortex zone rotation), we consider some uniform coordinate transformation $r\rightarrow\varepsilon r$ of the extremal solution of Eq. (12) (similar to that made in Ref. [19] for the dipole vortex solution). Under this transformation, the functional F on the extremal solution does not change its value, while the angular momentum, the mass, and the potential part of the energy are proportional to ε^2. The kinetic part of the energy also does not change its value and, therefore, the variations of particular Lyapunov functional does not diverge. Thus we obtain the self-consistent condition to determine the angular velocity Ω_N of the extremal vortex distribution

$$\Omega_N=\frac{\frac{1}{2}\int(|\Psi|^2-1)^2d^2r}{NM-(\vec{M})_z}. \tag{13}$$

It is worthwhile to note that this value of Ω_N is indeed determined only by the distribution of vortices inside and in the vicinity of the potential well. Indeed, according to the approximate form of the dark soliton (7), both the potential part of energy $(|\Psi|^2-1)^2\sim 1/r^4$ and the combination

$$\rho N-\rho rV_\theta=\rho(N-\phi'_\theta)\rightarrow 0, \tag{14}$$

decrease quickly outside the vortex zone where the field Ψ tends to have the phase $\phi\rightarrow N\theta$.

According to Eq. (13), the value Ω_N of the angular velocity of the self-consistent rotation of the vortex zone depends on the density level $|\Psi|^2$ in this region. A small level of the density gives a large value of Ω_N because both the mass integral and the angular momentum are proportional to this density. But the large velocity of the angular rotation of the vortex zone with finite size corresponds to a large azimuthal velocity that may exceed the speed of sound and produce Cherenkov radiation. Thus the breakup of the multicharged dark soliton and the development of the turbulent motion results in the appearance of some mass in the potential well in order to increase the density level $|\Psi|^2$ and to remove the Cherenkov radiation.

We now proceed to obtain simple criteria on the most stable vortex distribution within the vortex zone. To this end, we substitute the extremal solution (12) into the functional (11). Taking into account Eq. (13) in the resulting expression, this leads to the result

$$F=\tfrac{1}{2}\int(\nabla\Psi)^2d^2r=\tfrac{1}{2}\int(1-|\Psi|^4)d^2r. \tag{15}$$

Again, the divergence of F can be eliminated by calculating the difference between this functional and the one on the multicharged dark soliton with the asymptotic form (7) at

infinity. Equation (15) indicates that the functional F has a minimum if the nonlinear part of the potential energy

$$\int |\Psi|^4 d^2r = \int \rho(U+1)d^2r \tag{16}$$

has a maximum in the vortex zone. Since the density fluctuations $|\Psi|^2$ lead to an increase of the nonlinear part of the potential energy, the nonuniform density profile between the orbits of vortices arises in order to provide a more stable vortex distribution. It should also be noted that there is another interpretation of stable vortex distribution which is due to the minimum of the integral (15)

$$\int (\nabla\Psi)^2 d^2r = \int \rho\vec{V}^2 + (\nabla\rho^{1/2})^2 d^2r, \tag{17}$$

This integral is mainly determined by the kinetic energy of the vortices.

Equations (12) and (13) for the extremal distribution of vortices and for the self-consistent rotation of the vortex zone are the exact ones. As a final point, we point out that we can obtain the approximate extremal solution of Eq. (12), which describes a stable vortex distribution, and compare this solution with the results of numerical simulation. To do this analytically, we consider the mean-field approximation corresponding to the absence of azimuthal fluctuations of the density $|\Psi|^2$. This leads to a zero width of the vortex orbits. We also assume, as before, in obtaining the steady state solution of the linearized equation (9), that the phase (or velocity potential ϕ) of the extremal field Ψ between the orbits k and $(k+1)$ is determined only by the total number S_k of vortices on *inner* orbits. In this case the nonlinear term in Eq. (12) is small in the vortex zone; hence the corresponding nonlinear interaction (which leads to some finite level of the radial fluctuations of $|\Psi|^2$) is also small. Taking into account this phase dependence $\phi = S_k\theta$, we obtain the extremal solution

$$\Psi_e(\vec{r},t) = \Psi(r)\exp(iS_k\theta), \quad S_k = \sum_{j=0 \div k} N_j \tag{18}$$

between the orbits k and $k+1$. Then Eq. (12) yields the equation for the radial dependence of the amplitude $\Psi(r)$,

$$\frac{1}{2r}(r\Psi')' + \left\{1 + \Omega_N(N - S_k) - |\Psi|^2 - \frac{S_k^2}{2r^2}\right\}\Psi = 0, \tag{19}$$

where Ω_N is determined self-consistently by condition (13). Vortex orbits are located in zeros of the function $\Psi_e(\vec{r},t)$. Because Eq. (19) has a second derivative term, a smooth behavior of $\Psi(r)$ in these zeros is necessary. The nonlinear term in Eq. (19) is used to obtain the correct asymptotic form (7) only *outside* the vortex zone, and to obtain the density level inside the vortex zone.

Figure 5 demonstrates the solution $\Psi(r)$ of Eq. (19) for $N=17$ for the value of the angular velocity $\Omega_N = 1/N$ at the boundary of the vortex zone. One can see the coincidence of all orbit positions (zeros of Ψ) with those indicated in Fig. 3.

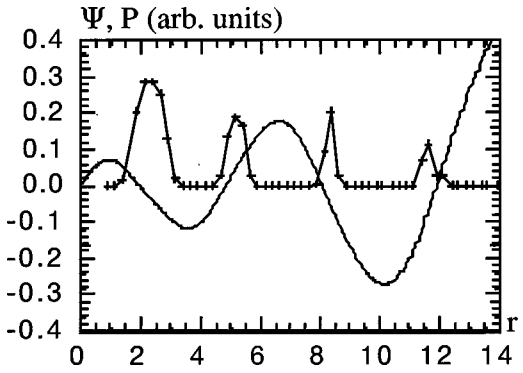

FIG. 5. The solution $\Psi(r)$ of Eq. (19) for the approximate extremal distribution of $N=17$ vortices (smooth curve) vs radius r. The positions of the zeros of this function were found to coincide with the numerically obtained maxima of the probability P to detect the vortex at the position r (curve with + signs from Fig. 2).

Thus the rotation of the vortex zone with some angular velocity can remove the deviation in the orbital positions found.

III. SUMMARY

The steady state turbulence of singly charged dark solitons corresponding to topologically stable solutions of the NLS equation has been analyzed both analytically and numerically. This turbulence arises after the breakup of a multicharged dark soliton with a topologically unstable structure. The turbulent motion of the singly charged dark solitons has both features of the motion of radiating vortices in gas dynamics (or radiating charges in electrodynamics) and quantum properties. The number of dark solitons (vortices) can define such turbulent motion completely.

We found that this turbulent motion is characterized by the formation of stable vortex orbits in the potential well of the primary multicharged dark soliton. These orbits are separated distinctly and have a finite width. The distances between the orbits are approximately constant. No vortices can move through the boundary of the potential well of the primary multicharged dark soliton during the long time evolution studied. We found that the turbulent distributions of the vortices do not depend on the size of the container when its radius is larger than the size of the potential well of the primary multicharged dark soliton. This can be explained by the existence of the ''extraordinary'' quantum term in the state equation (3) which determines the characteristic quantum length.

The distribution of singly charged dark solitons on these ''quantum'' orbits can be explained by means of a gas dynamic analogy. That is, the vortices in the particular steady turbulent distribution cannot be in Cherenkov resonance with sound waves, to prevent the radiation of energy from the vortex zone. Thus azimuthal velocities of vortices cannot exceed the speed of sound. This gives a constant number of dark solitons on each ''quantum'' orbit, in contrast to the uniform rotation of the separate hydrodynamic vortices. The particular distribution is similar to the model of the ''vortex atom'' with the Pauli exclusion principle for vortices due to a small probability of short distances between them. Indeed, neighboring vortices will quickly radiate energy, and diverge

to some finite distance on the order of the quantum healing length.

Classic linear waves with wavelengths greater than the healing length cannot be radiated outside the vortex zone due to reflection from the potential well that determines the size of the vortex zone. Moreover, the distribution of the vortices found describes the lowest (ground) quantum level of the particular problem [i.e., the state with the minimum value of the free energy (11)]. Thus the radiation outside the vortex zone can be adiabatically prohibited, similar to the absence of radiation from the distribution of the electrons in the ground level of a stable atom. This may explain the numerically observed stability of the vortex distributions during their long-time evolution.

Thus the main reason for the difference between the stable vortex distribution *rotating with constant azimuthal velocity* obtained in the present paper and the *constant vorticity* distribution in the form of infinite or finite lattices [13–15] is the distance between the vortices. In our case this distance is of the order of the healing length, the vortices are *nonseparated*, and the radiating effects are most important. But in the opposite case of a grid of *separate* vortices (as in a rotating container with He II), the *constant vorticity distribution* is only determined by an external parameter—the angular velocity of the container.

We found a simple criterion for the most stable *turbulent* distribution of particular chaotically moving, nonseparate vortices. The analysis is based on nontrivial extremal solutions of the Lyapunov functional. This functional corresponds to the energy integral in some self-consistently rotating coordinate system. The angular velocity of this rotation depends only on the vortex distribution, and does not correspond to a container rotation as it does in the case of separate hydrodynamic vortices in superfluid helium. Then the criterion of the most stable distribution corresponds to the maximum of the potential energy with respect to the background. The approximate solution of these extremal distributions, in the framework of an axially symmetric model (corresponding to the mean-field approximation), demonstrates the good agreement of the orbital positions with those obtained from direct numerical simulation of the NLS equation. But there are some discrepancies both between the predicted and calculated angular velocities and the density level within the vortex zone. These discrepancies arise due to correlations and fluctuations of the vortices, which have not been taken into account in the simplified axially symmetric model and require careful investigations.

ACKNOWLEDGMENTS

The authors are grateful to K.V. Chukbar and V.V. Yankov for useful discussions. We are also grateful to Bo Thidé for his help in performing the numerical simulations on the Lufsen Work Station. One of the authors (I.A.I.) would like to acknowledge the hospitality of the Department of Space and Plasma Physics at Uppsala University, and for providing excellent conditions for collaboration. This work was partially supported by the Russian State Program ''Fundamental Problems of Nonlinear Dynamics,'' and by the ''Russian Fund of Fundamental Researches'' (Grant No. 98-02-17174a). This work was supported by the European Communities under an Association Contract between EURATOM and the Swedish Natural Science Research Council (NFR) under Grant Nos. F-FU 10700-302, F-AC/FF 10700-303, and F-AA/FU 06481-309.

[1] H. C. Yuen and B. M. Lake, in *Solitons in Action*, edited by K. Lonngrén and A. Scott (Academic, New York, 1978).
[2] C. F. Jones and P. H. Roberts, J. Phys. A **15**, 2599 (1982).
[3] C. Josserand and Y. Pomeau, Europhys. Lett. **30**, 43 (1995).
[4] R. J. Donelly, *Quantized Vortices in Helium II* (Cambridge University Press, Cambridge, 1991).
[5] M. H. Anderson, J. R. Ensher, M. R. Matthews, C. E. Wieman, and E. A. Cornell, Science **269**, 198 (1995).
[6] V. E. Zakharov and A. B. Shabat, Zh. Éksp. Teor. Fiz. **64**, 1627 (1973) [Sov. Phys. JETP **37**, 823 (1973)].
[7] I. A. Ivonin and V. V. Yankov, Zh. Éksp. Teor. Fiz. **103**, 107 (1993) [JETP **76**, 57 (1993)].
[8] V. I. Petviashvili and V. V.Yankov, in *Reviews of Plasma Physics*, edited by B. B. Kadomtsev (Consultant Bureau, New York, 1989), Vol. 14.
[9] I. A. Ivonin, Zh. Éksp. Teor. Fiz. **107**, 1350 (1995) [Sov. Phys. JETP **80**, 750 (1995)].
[10] E. A. Kuznetsov and S. K. Turitsyn, Zh. Éksp. Teor. Fiz. **94**, 119 (1988) [Sov. Phys. JETP **67**, 1583 (1988)].
[11] H. Lamb, *Hydrodynamics*, 6th ed. (Dover, New York, 1945).
[12] I. A. Ivonin, Zh. Éksp. Teor. Fiz. **85**, 2252 (1997) [JETP **85**, 1233 (1997)].
[13] V. K. Tkachenko, Zh. Éksp. Teor. Fiz. **49**, 1875 (1966) [Sov. Phys. JETP **22**, 1282 (1966)].
[14] L. J. Cambell and R. M. Ziff, Phys. Rev. B **20**, 1886 (1979).
[15] L. J. Cambell, Phys. Rev. A **24**, 514 (1981).
[16] I. A. Ivonin, Fiz. Plazmy **18**, 581 (1992) [Sov. J. Plasma Phys. **18**, 302 (1992)].
[17] J. Neu, Physica D **43**, 385 (1990); **43**, 407 (1990).
[18] I. M. Gryanik, Izv., Acad. Sci., USSR, Atmos. Oceanic Phys. **19**, 203 (1983).
[19] E. A. Kuznetsov and J. J. Rasmussen, Phys. Rev. E **51**, 4479 (1995).